



Research Paper

Dosimetrics and radiomics-based prediction of pneumonitis after radiotherapy and immune checkpoint inhibition: The relevance of fractionation

Kim Melanie Kraus^{a,b,c,*}, Maksym Oreshko^{a,d}, Julia Anne Schnabel^{e,f,g}, Denise Bernhardt^{a,c},
Stephanie Elisabeth Combs^{a,b,c}, Jan Caspar Peeken^{a,b,c}

^a Department of Radiation Oncology, School of Medicine and Klinikum rechts der Isar, Technical University of Munich (TUM), 81675 Munich, Germany

^b Institute of Radiation Medicine (IRM), Helmholtz Zentrum München (HMGU) GmbH, German Research Center for Environmental Health, 85764 Neuherberg, Germany

^c Partner Site Munich, German Consortium for Translational Cancer Research (DKTK), 80336 Munich, Germany

^d Medical Faculty, University Hospital, LMU Munich, 80539 Munich, Germany

^e School of Biomedical Engineering and Imaging Sciences, King's College London, London, United Kingdom

^f School of Computation, Information and Technology, Technical University of Munich, Germany

^g Institute of Machine Learning in Biomedical Imaging, Helmholtz Zentrum München (HMGU) GmbH, German Research Center for Environmental Health, 85764 Neuherberg, Germany



ARTICLE INFO

Keywords:

Dosimetrics

Radiomics

Machine learning-based prediction

Radiation pneumonitis

Lung cancer

Immune checkpoint inhibition

ABSTRACT

Objectives: Post-therapy pneumonitis (PTP) is a relevant side effect of thoracic radiotherapy and immunotherapy with checkpoint inhibitors (ICI). The influence of the combination of both, including dose fractionation schemes on PTP development is still unclear. This study aims to improve the PTP risk estimation after radio(chemo)therapy (R(C)T) for lung cancer with and without ICI by investigation of the impact of dose fractionation on machine learning (ML)-based prediction.

Materials and Methods: Data from 100 patients who received fractionated R(C)T were collected. 39 patients received additional ICI therapy. Computed Tomography (CT), RT segmentation and dose data were extracted and physical doses were converted to 2-Gy equivalent doses (EQD2) to account for different fractionation schemes. Features were reduced using Pearson intercorrelation and the Boruta algorithm within 1000-fold bootstrapping. Six single (clinics, Dose Volume Histogram (DVH), ICI, chemotherapy, radiomics, dosimetrics) and four combined models (radiomics + dosimetrics, radiomics + DVH + Clinics, dosimetrics + DVH + Clinics, radiomics + dosimetrics + DVH + Clinics) were trained to predict PTP. Dose-based models were tested using physical dose and EQD2. Four ML-algorithms (random forest (rf), logistic elastic net regression, support vector machine, logitBoost) were trained and tested using 5-fold nested cross validation and Synthetic Minority Oversampling Technique (SMOTE) for resampling in R. Prediction was evaluated using the area under the receiver operating characteristic curve (AUC) on the test sets of the outer folds.

Results: The combined model of all features using EQD2 surpassed all other models (AUC = 0.77, Confidence Interval CI 0.76–0.78). DVH, clinical data and ICI therapy had minor impact on PTP prediction with AUC values between 0.42 and 0.57. All EQD2-based models outperformed models based on physical dose.

Conclusions: Radiomics + dosimetrics based ML models combined with clinical and dosimetric models were found to be suited best for PTP prediction after R(C)T and could improve pre-treatment decision making. Different RT dose fractionation schemes should be considered for dose-based ML approaches.

1. Introduction

R(C)T is standard of care for locally advanced lung cancer treatment.

The main dose limiting factor for thoracic RT is radiation induced lung injury, which reveals as PTP four to twelve weeks after RT and as lung fibrosis after months. The incidence of PTP is strongly dose dependent

* Corresponding author at: Department of Radiation Oncology, School of Medicine and Klinikum rechts der Isar, Technical University of Munich (TUM), Ismaninger Straße 22, 81675 Munich, Germany.

E-mail address: kimmelmanie.kraus@mri.tum.de (K.M. Kraus).

<https://doi.org/10.1016/j.lungcan.2024.107507>

Received 25 April 2023; Received in revised form 8 December 2023; Accepted 14 February 2024

Available online 17 February 2024

0169-5002/© 2024 The Authors. Published by Elsevier B.V. This is an open access article under the CC BY-NC license (<http://creativecommons.org/licenses/by-nc/4.0/>).

and increases with increasing fraction dose and known DVH-based variables such as mean lung dose and lung volume receiving more than 20 Gy.

Immunotherapy with ICI has essentially advanced lung cancer treatment by improvement of overall survival and local tumor control [1]. Consolidation immunotherapy after RCT for unresectable locally advanced non-small cell lung cancer (NSCLC) has become the standard of care. However, the combination of RT with immunotherapy has generated a gap of knowledge and an uncertainty in management of side effects, since some side effects as PTP may originate from both RT and ICI therapy due to interfering biological effects. Whereas the current data suggest no increase of severe pneumonitis due to the combination, there is evidence of increased all-grade pneumonitis [1–3]. The optimal effective and safe dose and fractionation schemes for radio-immunotherapy are yet unknown.

If PTP after RT and ICI therapy is diagnosed early, ultimate lung tissue damage can be prevented by immediate administration of corticosteroids and, depending on the etiology, discontinuation of ICI therapy. Thus, pre-treatment PTP prediction could support treatment decision making regarding dose and dose fractionation schemes in order to prevent PTP.

Even though lung radiation dose is the most important risk factor for PTP development [4], dosimetric data from DVHs alone cannot account for the spatial distribution of dose. With advancement of ML in medical applications, prediction of numerous clinical endpoints such as survival, local tumor control, disease progression, tumor detection and the occurrence of side effects has been investigated [5–13].

The improvement of PTP prediction after RT by adding quantitative analysis of spatial features from the CT image and the dose distribution, referred to as radiomics or dosiomics, respectively, has been proven [14–18]. Prediction could even be improved by the combination of radiomics and dosiomics analysis [19–21]. However, all these studies investigated PTP prediction after RT or RCT. There is less evidence regarding radioimmunotherapy. In two retrospective studies, radiomics was tested to reveal the etiology of pneumonitis [22,23] and was found to be useful for differentiation in cases of non-conclusive radiological judgement. In a multicenter prospective trial, Tohidinezhad et al. confirmed the above mentioned findings [24].

Whereas the majority of studies investigates dosiomics analysis based on physical dose, there are only sparse data on the effect of dose fractionation on PTP prediction. In this study, we aim to investigate the impact of combined R(C)T with ICI therapy and of dose fractionation on

the ML prediction of PTP.

2. Methods

2.1. Patient clinical factors

We analyzed data from $n = 100$ lung cancer patients, who received normo- and hypofractionated R(C)T between 2010 and 2021 as depicted in Fig. 1. Out of these, 39 patients received additional ICI therapy. In total, 38 patients were diagnosed with PTP, 20 of whom received additional ICI therapy as indicated in Table 1. The majority of 89 patients had stage IV lung cancer and 46 patients were treated in curative intent. From the 39 patients, who received additional ICI therapy, 17 received Durvalumab maintenance therapy, 9 received Pembrolizumab, 7 Atezolizumab and 6 Nivolumab. Patient characteristics included age, sex, Karnofsky performance index (KPI), tumor location, planning target volume size, former or concomitant chemotherapy and ICI therapy status. RT fractionation schemes varied with single doses ranging from 1.8 Gy to 3.0 Gy and total doses from 30 Gy to 66 Gy. The occurrence of PTP was monitored based on clinical factors (coughing, dyspnea, pleural pain) from patient records and follow-up CTs and was graded according to the Common Terminology Criteria for Adverse Events version 5.0 [25].

2.2. Volumetric CT and dose data

Patients received a 4DCT prior to RT, which was used for definition of RT segmentation data. These data, together with dosimetric data including the mean lung dose, and the lung volume receiving at least 5 Gy (V5), V10, V15, V20, V30, V40, V50, accordingly, were extracted from the treatment planning system and further processed using the open source platform 3D Slicer [2] and the radiotherapy toolkit [3]. Details on the method have been published previously [26] and are depicted in Fig. 2. In brief, the gross tumor volume (GTV) was defined on simulation CTs. During treatment planning an internal target volume (ITV) was defined and a planning target volume (PTV) was created by adding an isotropic margin of 5 mm.

In order to analyze the impact of dose fractionation, physical doses were converted to EQD2 according to equation (1) based on the Linear Quadratic Model (LQM) [27], where D is the sum physical dose over all fractions, d is the fraction dose, and α/β is equal to 3 for lung tissue.

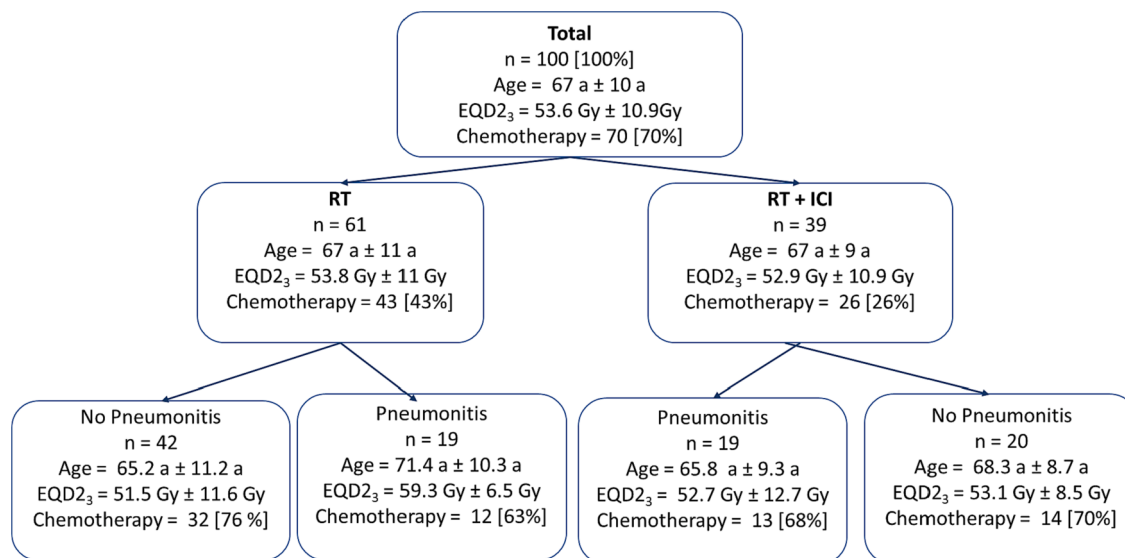


Fig. 1. Patient data. Patient mean age and standard deviations are provided. Prescription doses are given in mean values and standard deviations of 2 Gy-equivalent doses for an α/β of 3 Gy (EQD_{2,3}). The number of patients who received prior or concomitant chemotherapy is provided.

Table 1
Patient characteristics.

Characteristic	Value	Value [%]
n	100	100
Age [a]		
Mean ± SD	67 ± 10	
Range	43–90	
Sex		
Male	73	73
Female	27	27
KPI		
Mean ± SD	94 ± 9	
Range	50–100	
GTV size [mm³]		
Mean ± SD	201.0 ± 352.4	
Range	1.3–3190.0	
Location		
Right upper lobe	2	
Right middle lobe	27	
Right lower lobe	20	
Left upper lobe	18	
Left lower lobe	9	
Right central	16	
Left central	8	
RT + ICI		
Yes	39	39
No	61	61
prior/concomitant Chemotherapy		
Yes	70	70
No	30	30
Stage		
I	0	0
II	9	9
III	48	48
IV	43	43
Treatment Intent		
curative	46	46
palliative	54	54
Pneumonitis		
Yes	38	38
No	62	62

$$EQD2 = D \left[\frac{d + \frac{\alpha}{\beta}}{2 + \frac{\alpha}{\beta}} \right] \tag{1}$$

2.3. Feature processing

Quantitative features from volumetric CT and volumetric RT dose data with Gy values treated as grey-levels (physical dose vs. EQD2) were extracted using the open-source library Pyradiomics in python [28,29]. For each volume of interest (lungs minus GTV, PTV + 2 cm, ipsilateral lung minus GTV), 104 radiomics and dosiomics features were extracted, respectively, leading to 312 features in total. Details on the feature extraction can be found in a previous study [26]. All 104 features used for feature extraction and the reduced extracted features for all models tested are provided in Supplement Tables 1 and 2, respectively. Feature reduction was conducted within 1000-fold bootstrapping combining Pearson-intercorrelation coefficient (cut-off 0.7) and the Boruta algorithm. For each bootstrap run the number of selected features and the selected features were recorded. The optimal number of features “n” was defined as the median number of selected features over all bootstrap runs. Finally, the top “n” listed features over all bootstrapping runs were selected for final model building.

2.4. Machine learning models

Six single predictive models (radiomics, dosiomics, clinics, DVH, chemotherapy, ICI) and five combinations (dosiomics + radiomics, DVH + clinical factors, radiomics + DVH + clinical data, dosiomics + DVH + clinical factors, all) were tested using different ML algorithms including random forest (rf), logistic elastic net regression (glmnet), support vector machine (svmRadial), and logitBoost. The clinical model also included ICI and chemotherapy and were tested as single models, additionally. The ML prediction method has been described in detail [26], [30] and included 100 iterations of 5-fold nested cross validation [6], Synthetic Minority Oversampling Technique (SMOTE) resampling based on the R DMwR package to overcome class imbalance [31], and hyperparameter optimization using grid search (see Supplemental

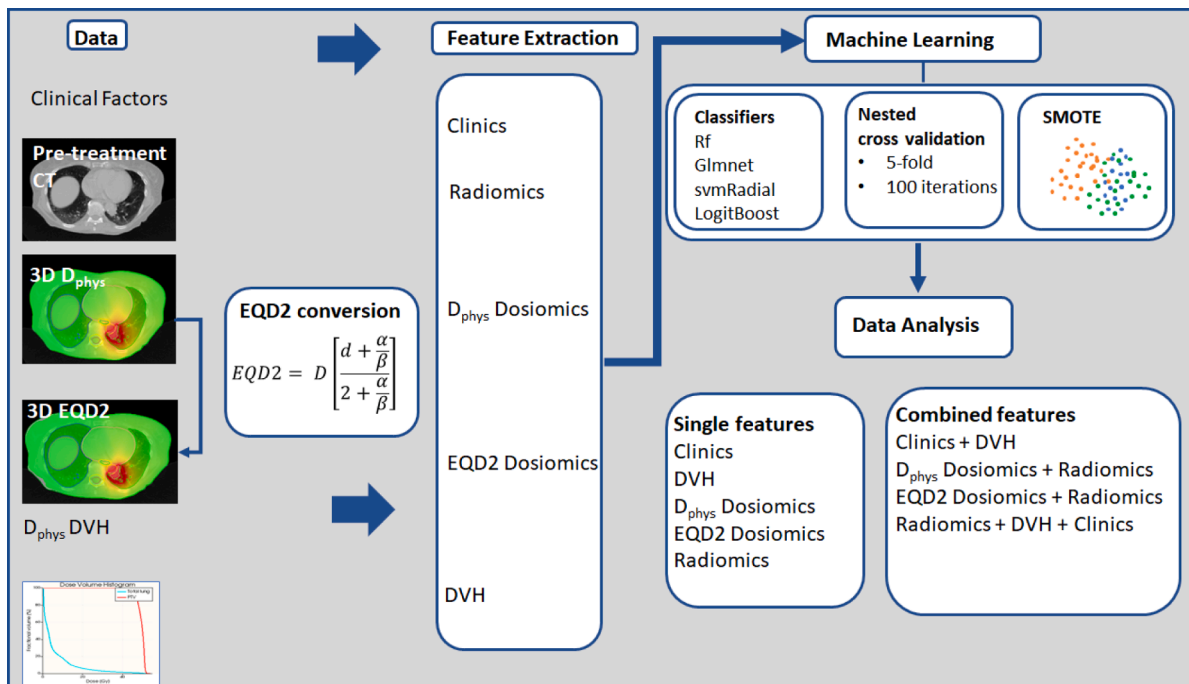


Fig. 2. Workflow. Physical Doses D_{phys} are converted to 2-Gy equivalent doses (EQD2).

Table 3 for hyperparameter spaces and supplementary section 4 for calibration curves). Thus, within the 5-fold nested cross validation approach, the patient cohort was divided by 80:20 training/test patient ratio for the outer fold and 64/16 patients for the inner folds. Single feature models (ICI, DVH, chemotherapy) were tested using logistic regression and ICI and chemotherapy were additionally added into the clinical model. All other dose-based models were simulated twice with physical dose and EQD2 separately, leading to differing results also for non-dose based models. The predictive ability for each model and combinations were evaluated by the mean AUC on the test sets of the outer fold and a confidence interval with a confidence level of 95 %. AUC values were ranked for the four different models applied. Box and scatterplots are presented with each point representing the result of one outer validation fold.

We present the results of the following article in accordance with the transparent reporting of a multivariable prediction model for individual prognosis or diagnosis (TRIPOD). A corresponding TRIPOD statement can be found in the Supplementary Material Table 5.

3. Results

3.1. Classifiers

Comparing different classifiers revealed rf to perform best as depicted by AUC values ranked from 1 to 4 for the four different classifiers in Fig. 3. Fig. 4 shows all AUC values for all classifiers and shows the range of between 0.46 for not predictive models such as clinics and the combination of clinics and DVH features, and 0.77 for top performing models such as the combination of dosiomics and radiomics together with clinical and DVH models. Due to these findings, rf was chosen for all following analyses in this study. Models that might be impacted by shape features, were also run without shape features to quantify their influence. No specific trend was observed and results are presented in the supplementary material section 6.

3.2. Feature extraction

In total, five clinical features were extracted and ranked such as age, tumor size, tumor location, sex, and KPI. From DVH features, only V50 was extracted from the EQD2 and physical dose features. The combined models resulted in the same features of both individual models together. The other models resulted in 19 to 39 and 21 to 40 features for physical dose and EQD2, respectively, as listed in Table 2.

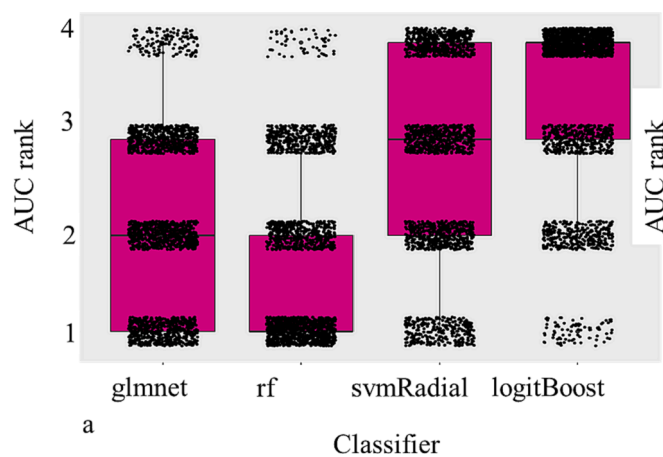


Fig. 3. Box and Scatterplots showing area under the receiver operating characteristic curves (AUCs) ranked values (lower being better) for different classifiers used over all datasets and repetitions.

3.3. Machine learning PTP prediction

All investigated models predicted PTP better than random (AUC > 0.5) using rf classifier as depicted in Table 3, apart from the chemotherapy model (AUC = 0.42) and ICI model (AUC = 0.45). Across all results, the combination of all models performed best (AUC = 0.77 (0.76–0.78)) for EQD2, followed by dosiomics + radiomics (AUC = 0.76 (0.75–0.77)) and dosiomics + DVH + Clinics (AUC = 0.69 (0.68–0.7)) as depicted in Table 3. The addition of other features such as DVH and clinical factors slightly improved the predictive performance. Compared to all physical dose models, PTP prediction of EQD2 models was superior. For physical dose models, the combined model of Radiomics + DVH + Clinics performed best (AUC = 0.69 (0.68–0.70)). For the single models, Radiomics resulted in the highest predictive value (AUC = 0.68 (0.67–0.69)).

Patient clinical factors model performed worse and was slightly better than random with AUC = 0.52 (0.62–0.53) for EQD2 and physical dose. ICI therapy had no impact on PTP prediction with AUC = 0.45 (0.44–0.46) for both, EQD2 and physical dose.

4. Discussion

Our results show the impact of dose fractionation on the volumetric dose-based ML prediction of PTP after RCT. Concomitant ICI therapy did not influence PTP prediction.

Like in previous studies, our results reveal good predictive capability of dosiomics-based prediction models with an AUC of 0.68 for EQD2. The study of Liang et al. revealed slightly better results with an AUC value of 0.78 for dosiomics feature analysis, which was superior to normal tissue risk model and dosimetric feature analyses [17]. In our study, predictive capability could even be improved by combining dosiomics with radiomics based models, indicated by an AUC value of 0.67 and 0.76 for physical dose and EQD2, respectively. These findings are well in line with the current evidence from literature. In two similar approaches, AUC values of 0.68 and 0.88 for the combination or radiomics and dosiomics feature models were found [19,32]. Jiang et al. even found improved prediction for a combination of radiomics, dosiomics, age, and T stage models with an AUC value of 0.94 for prediction of acute radiation pneumonitis after RCT for lung cancer [18]. In a combination of retrospective and prospective data cohort of lung cancer patients, Zhang et al. recently confirmed best predictive results for the combination of radiomics and dosiomics with clinical parameters [20].

Compared to the above-mentioned studies, our approach gained additional value by analyzing the impact of different fractionation schemes on PTP prediction. As has been shown before, the fraction dose is an important risk factor for the development of pneumonitis [4]. We found all dose-based prediction models to result in improved prediction for EQD2 doses, indicating that fractionation should be considered for dose-based prediction strategies. Similar findings have been demonstrated by Zhou et al. [33], who investigated the influence of fraction doses of 1.5 Gy to 2.75 Gy on the prediction of radiation pneumonitis \geq grade 1 based on 91 NSCLC patients. The authors found significant improvement when an EQD2-based dosiomics was applied.

Another aspect of this study focused on the influence of ICI therapy on pneumonitis prediction for combined radioimmunotherapy. With increasing use of immunotherapy for lung cancer treatment, interference of immunological and radiation induced biological effects become relevant with regard to side effects. Whereas data from clinical trials point to no increased risk for severe pneumonitis after R(C)T and consolidation ICI therapy, there might be an increased risk for all-grade pneumonitis with impact on clinical decision making [2,3,34]. Moreover, differentiation between radiation-induced or ICI therapy-related PTP is challenging due to similar radiological features. However, distinction between these could influence clinical management. Thus, differentiation between the etiology of the PTP, as well as pre-treatment PTP risk prediction can be of importance for practical clinical decision

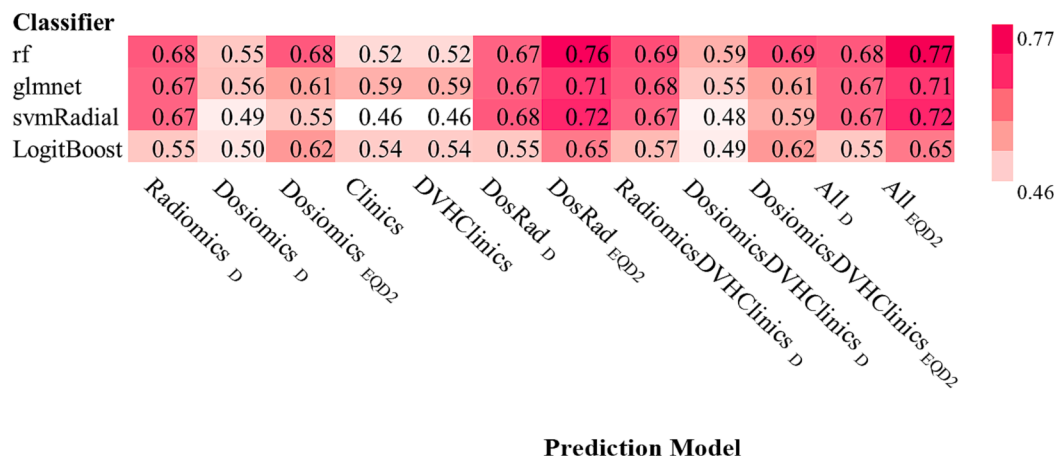


Fig. 4. Area under the receiver operating characteristic curves (AUC) values for all classifiers and models tested. Subscripted D and EQD2 refer to physical dose and 2 Gy-equivalent dose (EQD2), respectively. Darker colors indicate higher AUC values and better prediction performance.

Table 2

Top three features ranked in the order of frequency and the frequency, with which they have been selected after feature reduction for all models, that have been processed by feature reduction. Subscripted D and EQD2 refer to physical dose and 2 Gy-equivalent dose (EQD2), respectively. CT refers to CT-based features, D refers to dose-based features, PTV refers to planning target volume, IL to ipsilateral lung and TL to total Lung.

Model	Ranked reduced features	Frequency
Radiomics _D	CT_PTV_ngtdm_Strength	765
	CT_IL_shape_Sphericity	690
	CT_IL_glcml_Icn	629
Dosiomics _D	D_TL_firstorder_InterquartileRange	640
	D_PTV_gldm_DependenceNonUniformityNormalized	626
	D_TL_shape_Sphericity	609
Dosiomics _{EQD2}	D_PTV_glszm_GrayLevelNonUniformity	657
	D_PTV_glrml_RunEntropy	560
	D_IL_shape_Sphericity	553
Radiomics _D + Dosiomics _D	CT_PTV_ngtdm_Strength	754
	CT_IL_glcml_Icn	617
	CT_PTV_glcml_ClusterProminence	587
Radiomics _{EQD2} + Dosiomics _{EQD2}	CT_PTV_ngtdm_Strength	750
	D_PTV_glszm_GrayLevelNonUniformity	632
	CT_IL_glcml_Icn	607
Radiomics _D + Clinics _D + DVH _D	CT_PTV_ngtdm_Strength	
	CT_IL_shape_Sphericity	
	CT_IL_glcml_Icn	
Radiomics _{EQD2} + Clinics _{EQD2} + DVH _{EQD2}	CT_PTV_ngtdm_Strength	
	CT_IL_shape_Sphericity	
	CT_IL_glcml_Icn	
Dosiomics _D + Clinics _D + DVH _D	D_TL_firstorder_InterquartileRange	
	D_PTV_gldm_DependenceNonUniformityNormalized	
	D_TL_shape_Sphericity	
Dosiomics _{EQD2} + Clinics _D + DVH _D	D_PTV_glszm_GrayLevelNonUniformity	
	D_PTV_glrml_RunEntropy	
	D_IL_shape_Sphericity	
Radiomics _D + Dosiomics _D + Clinics _D + DVH _D	CT_PTV_ngtdm_Strength	
	CT_IL_glcml_Icn	
	CT_PTV_glcml_ClusterProminence	
Radiomics _{EQD2} + Dosiomics _{EQD2} + Clinics _{EQD2} + DVH _{EQD2}	CT_PTV_ngtdm_Strength	
	PTV_glszm_GrayLevelNonUniformity	
	CT_IL_glcml_Icn	

making. In previous works, CT-based radiomics models have been found capable to differentiate between radiation- and ICI-induced PTP with AUC values ≥ 0.76 [22–24]. Chen et al. revealed radiological differences of these etiologies and found bilateral PTP extension, including at least 3 lobes, to be characteristic for ICI-associated PTP [22]. In a multicenter prospective trial, Tohidinezhad et al. found the line of immunotherapy to be predictive for PTP development, indicating that the patients who received immunotherapy as the first-line treatment were at higher PTP risk [24].

Whereas the above-mentioned studies focused on the use of ML for differentiation between the etiology of PTP, our study investigated the

influence of ICI therapy on the occurrence of PTP. In this study, ICI therapy did not show a predictive value for the development of pneumonitis with an AUC value of 0.45. Previous and concomitant chemotherapy was not found to be predictive for PTP. As a consequence, patient-inherent anatomic-biological factors captured by CT-based radiomic features and the three-dimensional RT dose distribution are thought to be of higher relevance for the development of PTP.

Obvious limitations of our study include a limited amount of patient data. Development of ML models with a dataset of 100 is challenging, however we applied a multi-step approach to overcome these limitations including the following steps: 1) cross validation to obtain measures of

Table 3

AUC and 95 % confidence intervals (CI) for all investigated Machine Learning models for 2 Gy-equivalent doses (EQD2) and physical doses (D). Single feature models (ICI, DVH, Chemotherapy) were additionally tested using logistic regression. Models without dosiomics models were run only once (depicted under EQD2).

Model	95 % CI		D	
	AUC	EQD2		
Radiomics	0.68	(0.67–0.69)		
Dosiomics	0.68	(0.67–0.69)	0.55	(0.54–0.56)
Dosiomics + Radiomics	0.76	(0.75–0.77)	0.67	(0.66–0.68)
Clinical Factors	0.52	(0.51–0.53)		
DVH + Clinical Factors	0.52	(0.51–0.54)		
Radiomics + DVH + Clinics	0.69	(0.68–0.7)		
Dosiomics + DVH + Clinics	0.69	(0.686–0.7)	0.68	(0.67–0.69)
All	0.77	(0.76–0.78)	0.68	(0.67–0.69)
Chemotherapy	0.42	(0.41–0.42)		
ICI	0.45	(0.44–0.46)		
DVH	0.57	(0.56–0.58)		

statistical variance, 2) SMOTE to reduce the influence of imbalanced datasets, 3) multi-step feature reduction, 4) no beforehand feature number assumption, 5) nested-cross validation allowing for multiple testing on unseen datasets. However, our models were not tested on external datasets, which could have demonstrated the reproducibility and will be conducted in a future study.

As the patient dataset was rather small with an imbalance towards a smaller group receiving ICI therapy (39 vs. 61), we found increased pneumonitis rate in the RT + ICI group compared to the RT only group (50 % vs. 30 %). Obviously, the rates of pneumonitis are increased in both groups compared to the data from the literature, which is most likely due to the inclusion of all grades of pneumonitis in our study, whereas the majority of studies focusing on clinical data provide data only with pneumonitis grade ≥ 2 . We decided to investigate grade 1 pneumonitis as well to account for all, even if unknown, effects of combined radioimmunotherapy including different radiological features, as there is an indication that ICI therapy might lead to increased all-grade PTP [34,35].

5. Conclusions

We showed superiority of combined radiomics and EQD2-based dosiomics, together with clinical and dosimetric ML models for PTP prediction without an impact of ICI therapy. These results suggest to consider fractionation schemes for dose-based prediction strategies.

Author contributions

KMK and JCP designed the project. KMK and JCP wrote the paper. KMK and MO collected and analysed the data. Statistical analysis and ML modelling were conducted by KMK, MO, and JCP. JCP, DB, KMK and SEC provided expert clinical knowledge. All authors edited the manuscript.

Funding

KMK received funding for this project from the German Cancer Consortium (DKTK). This project was funded by the Deutsche Forschungsgemeinschaft (DFG, German Research Foundation) – 515279324 (JCP, JAS).

8. Ethics statement

The studies involving human participants were reviewed and approved by 466/16S. Written informed consent for participation was not required for this study in accordance with the national legislation and the institutional requirements.

CRedit authorship contribution statement

Kim Melanie Kraus: Conceptualization, Data curation, Formal analysis, Investigation, Supervision, Validation, Visualization, Writing – original draft, Writing – review & editing. **Maksym Oreshko:** Data curation, Formal analysis, Writing – review & editing. **Julia Anne Schnabel:** Funding acquisition, Investigation, Project administration, Writing – review & editing. **Denise Bernhardt:** Supervision, Writing – review & editing. **Stephanie Elisabeth Combs:** Supervision, Validation, Writing – review & editing. **Jan Caspar Peeken:** Conceptualization, Data curation, Formal analysis, Funding acquisition, Investigation, Methodology, Project administration, Supervision, Writing – review & editing.

Declaration of competing interest

The authors declare that they have no known competing financial interests or personal relationships that could have appeared to influence the work reported in this paper.

Appendix A. Supplementary data

Supplementary data to this article can be found online at <https://doi.org/10.1016/j.lungcan.2024.107507>.

References

- [1] S.J. Antonia, A. Villegas, D. Daniel, D. Vicente, S. Murakami, R. Hui, et al., Overall survival with durvalumab after chemoradiotherapy in stage III NSCLC, *N. Engl. J. Med.* 379 (2018) 2342–2350, <https://doi.org/10.1056/NEJMoa1809697>.
- [2] N. Shaverdian, A.E. Lisberg, K. Bornazyan, D. Veruttipong, J.W. Goldman, S. C. Formenti, et al., Previous radiotherapy and the clinical activity and toxicity of pembrolizumab in the treatment of non-small-cell lung cancer: a secondary analysis of the KEYNOTE-001 phase 1 trial, *Lancet Oncol.* 18 (2017) 895–903, [https://doi.org/10.1016/S1473-0165\(17\)30380-7](https://doi.org/10.1016/S1473-0165(17)30380-7).
- [3] M.S. Anscher, S. Arora, C. Weinstock, A. Amaty, P. Bandaru, C. Tang, et al., Association of radiation therapy with risk of adverse events in patients receiving immunotherapy: a pooled analysis of trials in the US Food and Drug Administration Database, *JAMA Oncol.* 8 (2022) 232–240, <https://doi.org/10.1001/jamaoncol.2021.6439>.
- [4] T.M. Briere, S. Krafft, Z. Liao, M.K. Martel, Lung size and the risk of radiation pneumonitis, *Int. J. Radiat. Oncol. Biol. Phys.* 94 (2016) 377–384, <https://doi.org/10.1016/j.ijrobp.2015.10.002>.
- [5] J.C. Peeken, B. Wiestler, S.E. Combs, Image-guided radiooncology: the potential of radiomics in clinical application, in: O. Schober, F. Kiessling, J. Debus (Eds.), *Molecular Imaging in Oncology*, Springer International Publishing, Cham, 2020, pp. 773–794.
- [6] S. Leger, A. Zwanenburg, K. Leger, F. Lohaus, A. Linge, A. Schreiber, et al., Comprehensive analysis of tumour sub-volumes for radiomic risk modelling in locally advanced HNSCC, *Cancers* 12 (2020) 3047, <https://doi.org/10.3390/cancers12103047>.
- [7] J.C. Peeken, M.A. Shouman, M. Kroenke, I. Rauscher, T. Maurer, J.E. Gschwend, et al., A CT-based radiomics model to detect prostate cancer lymph node metastases in PSMA radioguided surgery patients, *Eur. J. Nucl. Med. Mol. Imaging* 47 (2020) 2968–2977, <https://doi.org/10.1007/s00259-020-04864-1>.
- [8] J.C. Peeken, M. Bernhofer, M.B. Spraker, D. Pfeiffer, M. Devecka, A. Thamer, et al., CT-based radiomic features predict tumor grading and have prognostic value in patients with soft tissue sarcomas treated with neoadjuvant radiation therapy, *Radiother. Oncol.* 135 (2019) 187–196, <https://doi.org/10.1016/j.radonc.2019.01.004>.
- [9] J.C. Peeken, M.B. Spraker, C. Knebel, H. Dapper, D. Pfeiffer, M. Devecka, et al., Tumor grading of soft tissue sarcomas using MRI-based radiomics, *EBioMedicine* 48 (2019) 332–340, <https://doi.org/10.1016/j.ebiom.2019.08.059>.
- [10] I. Shahzadi, A. Zwanenburg, A. Lattermann, A. Linge, C. Baldus, J.C. Peeken, et al., Analysis of MRI and CT-based radiomics features for personalized treatment in locally advanced rectal cancer and external validation of published radiomics models, *Sci. Rep.* 12 (2022) 10192, <https://doi.org/10.1038/s41598-022-13967-8>.
- [11] D.M. Lang, J.C. Peeken, S.E. Combs, J.J. Wilkens, S. Bartzsch, Deep learning based HPV status prediction for oropharyngeal cancer patients, *Cancers* 13 (2021) 786, <https://doi.org/10.3390/cancers13040786>.
- [12] F. Navarro, H. Dapper, R. Asadpour, C. Knebel, M.B. Spraker, V. Schwarze, et al., Development and external validation of deep-learning-based tumor grading models in soft-tissue sarcoma patients using MR imaging, *Cancers* 13 (2021) 2866, <https://doi.org/10.3390/cancers13122866>.
- [13] O. Llorián-Salvador, J. Akhgar, S.U. Pigorsch, K.J. Borm, S. Münch, D. Bernhardt, et al., Machine learning based prediction of pain response to palliative radiation therapy - is there a Role for Planning CT-based Radiomics and Semantic Imaging

- Features? Preprints 2022 2022. <https://doi.org/10.20944/preprints202212.0195.v1>.
- [14] S.P. Krafft, A. Rao, F. Stingo, T.M. Briere, L.E. Court, Z. Liao, et al., The utility of quantitative CT radiomics features for improved prediction of radiation pneumonitis, *Med. Phys.* 45 (2018) 5317–5324, <https://doi.org/10.1002/mp.13150>.
- [15] D. Kawahara, N. Imano, R. Nishioka, K. Ogawa, T. Kimura, T. Nakashima, et al., Prediction of radiation pneumonitis after definitive radiotherapy for locally advanced non-small cell lung cancer using multi-region radiomics analysis, *Sci. Rep.* 11 (2021) 16232, <https://doi.org/10.1038/s41598-021-95643-x>.
- [16] V. Bourbonne, R. Da-Ano, V. Jaouen, F. Lucia, G. Dissaux, J. Bert, et al., Radiomics analysis of 3D dose distributions to predict toxicity of radiotherapy for lung cancer, *Radiother. Oncol.* 155 (2021) 144–150, <https://doi.org/10.1016/j.radonc.2020.10.040>.
- [17] B. Liang, H. Yan, Y. Tian, X. Chen, L. Yan, T. Zhang, et al., Dosiomics: extracting 3D spatial features from dose distribution to predict incidence of radiation pneumonitis, *Front. Oncol.* 9 (2019) 269, <https://doi.org/10.3389/fonc.2019.00269>.
- [18] W. Jiang, Y. Song, Z. Sun, J. Qiu, L. Shi, Dosimetric factors and radiomics features within different regions of interest in planning CT images for improving the prediction of radiation pneumonitis, *Int. J. Radiat. Oncol. Biol. Phys.* 110 (2021) 1161–1170, <https://doi.org/10.1016/j.ijrobp.2021.01.049>.
- [19] C. Puttanawarut, N. Sirirutbunkajorn, N. Tawong, C. Jiarpinitnun, S. Khachonkham, P. Pattaranutaporn, et al., Radiomic and dosiomic features for the prediction of radiation pneumonitis across esophageal cancer and lung cancer, *Front. Oncol.* 12 (2022) 768152, <https://doi.org/10.3389/fonc.2022.768152>.
- [20] Z. Zhang, Z. Wang, M. Yan, J. Yu, A. Dekker, L. Zhao, et al., Radiomics and dosiomics signature from whole lung predicts radiation pneumonitis: a model development study with prospective external validation and decision-curve analysis, *Int. J. Radiat. Oncol. Biol. Phys.* 115 (2023) 746–758, <https://doi.org/10.1016/j.ijrobp.2022.08.047>.
- [21] M. Yakar, D. Etiz, M. Metintas, G. Ak, O. Celik, Prediction of radiation pneumonitis with machine learning in stage III lung cancer: a pilot study, *Technol. Cancer Res. Treat.* 20 (2021), <https://doi.org/10.1177/15330338211016373>, 15330338211016373.
- [22] X. Chen, K. Sheikh, E. Nakajima, C.T. Lin, J. Lee, C. Hu, et al., Radiation versus immune checkpoint inhibitor associated pneumonitis: distinct radiologic morphologies, *Oncologist* 26 (2021) e1822–e1832, <https://doi.org/10.1002/onco.13900>.
- [23] J. Cheng, Y. Pan, W. Huang, K. Huang, Y. Cui, W. Hong, et al., Differentiation between immune checkpoint inhibitor-related and radiation pneumonitis in lung cancer by CT radiomics and machine learning, *Med. Phys.* 49 (2022) 1547–1558, <https://doi.org/10.1002/mp.15451>.
- [24] F. Tohidinezhad, D. Bontempi, Z. Zhang, A.-M. Dingemans, J. Aerts, G. Bootsma, et al., Computed tomography-based radiomics for the differential diagnosis of pneumonitis in stage IV non-small cell lung cancer patients treated with immune checkpoint inhibitors, *Eur. J. Cancer* 183 (2023) 142–151, <https://doi.org/10.1016/j.ejca.2023.01.027>.
- [25] Common Terminology Criteria for Adverse Events (CTCAE) | Protocol Development | CTEP 2022. https://ctep.cancer.gov/protocoldevelopment/electronic_applications/ctc.htm (accessed March 28, 2022).
- [26] Kraus KM, Oreshko M, Bernhardt D, Combs SE, Peeken JC. Dosiomics and radiomics to predict pneumonitis after thoracic stereotactic body radiotherapy and immune checkpoint inhibition. *Frontiers in Oncology* 2023;13.
- [27] S.J. McMahon, The linear quadratic model: usage, interpretation and challenges, *Phys. Med. Biol.* 64 (2018), <https://doi.org/10.1088/1361-6560/aaf26a>, 01TR01.
- [28] Radiomics n.d. <https://www.radiomics.io/index.html> (accessed November 23, 2022).
- [29] J.J.M. van Griethuysen, A. Fedorov, C. Parmar, A. Hosny, N. Aucoin, V. Narayan, et al., Computational radiomics system to decode the radiographic phenotype, *Cancer Res.* 77 (2017) e104–e107, <https://doi.org/10.1158/0008-5472.CAN-17-0339>.
- [30] T.M. Deist, F.J.W.M. Dankers, G. Valdes, R. Wijsman, I.-C. Hsu, C. Oberije, et al., Machine learning algorithms for outcome prediction in (chemo)radiotherapy: An empirical comparison of classifiers, *Med. Phys.* 45 (2018) 3449–3459, <https://doi.org/10.1002/mp.12967>.
- [31] N.V. Chawla, K.W. Bowyer, L.O. Hall, W.P. Kegelmeyer, SMOTE: synthetic minority over-sampling technique, *Jair* 16 (2002) 321–357, <https://doi.org/10.1613/jair.953>.
- [32] B. Li, X. Zheng, J. Zhang, S. Lam, W. Guo, Y. Wang, et al., Lung subregion partitioning by incremental dose intervals improves omics-based prediction for acute radiation pneumonitis in non-small-cell lung cancer patients, *Cancers* 14 (2022) 4889, <https://doi.org/10.3390/cancers14194889>.
- [33] L. Zhou, Y. Wen, G. Zhang, L. Wang, S. Wu, S. Zhang, Machine learning-based multiomics prediction model for radiation pneumonitis, *J. Oncol.* 2023 (2023) 5328927, <https://doi.org/10.1155/2023/5328927>.
- [34] S.J. Antonia, A. Villegas, D. Daniel, D. Vicente, S. Murakami, R. Hui, et al., Durvalumab after chemoradiotherapy in stage III non-small-cell lung cancer, *N. Engl. J. Med.* 377 (2017) 1919–1929, <https://doi.org/10.1056/NEJMoa1709937>.
- [35] K.M. Kraus, C. Bauer, B. Feueracker, J.C. Fischer, K.J. Borm, D. Bernhardt, et al., Pneumonitis after stereotactic thoracic radioimmunotherapy with checkpoint inhibitors: exploration of the dose–volume–effect correlation, *Cancers* 14 (2022) 2948, <https://doi.org/10.3390/cancers14122948>.